

Positronium laser cooling via the 1^3S – 2^3P transition with a broadband laser pulse

L. T. Glöggler,¹ N. Gusakova,^{1,2} B. Rienäcker,^{3,*} A. Camper,^{4,†} R. Caravita,^{5,‡} S. Huck,^{1,6} M. Volponi,^{1,7,5} T. Wolz,¹ L. Penasa,^{7,5} V. Krumins,^{1,8} F. Gustafsson,¹ M. Auzins,⁸ B. Bergmann,⁹ P. Burian,⁹ R. S. Brusa,^{7,5} F. Castelli,^{10,11} R. Ciuryło,¹² D. Comparat,¹³ G. Consolati,^{10,14} M. Doser,¹ L. Graczykowski,¹⁵ M. Grosbart,¹ F. Guatieri,^{7,5} S. Haider,¹ M. A. Janik,¹⁵ G. Kasprówicz,¹⁶ G. Khatri,¹ L. Kłosowski,¹² G. Kornakov,¹⁵ L. Lappo,¹⁵ A. Linek,¹² J. Malamant,⁴ S. Mariazzi,^{7,5} V. Petracek,¹⁷ M. Piwiński,¹² S. Pospisil,⁹ L. Povolo,^{7,5} F. Prelz,¹⁰ S. A. Rangwala,¹⁸ T. Rauschendorfer,^{1,19} B. S. Rawat,^{3,20} V. Rodin,³ O. M. Røhne,⁴ H. Sandaker,⁴ P. Smolyanskiy,⁹ T. Sowiński,²¹ D. Tefelski,¹⁵ T. Vafeiadis,¹ C. P. Welsch,^{3,20} M. Zawada,¹² J. Zielinski,¹⁵ and N. Zurlo^{22,23}

(The AEgIS collaboration)

¹*Physics Department, CERN, 1211 Geneva 23, Switzerland*

²*Department of Physics, NTNU, Norwegian University of Science and Technology, Trondheim, Norway*

³*Department of Physics, University of Liverpool, Liverpool L69 3BX, UK*

⁴*Department of Physics, University of Oslo, Sem Sælandsvei 24, 0371 Oslo, Norway*

⁵*TIFPA/INFN Trento, via Sommarive 14, 38123 Povo, Trento, Italy*

⁶*Institute for Experimental Physics, Universität Hamburg, 22607 Hamburg, Germany*

⁷*Department of Physics, University of Trento, via Sommarive 14, 38123 Povo, Trento, Italy*

⁸*University of Latvia, Department of Physics Raina boulevard 19, LV-1586, Riga, Latvia*

⁹*Institute of Experimental and Applied Physics, Czech Technical University in Prague, Husova 240/5, 110 00, Prague 1, Czech Republic*

¹⁰*INFN Milano, via Celoria 16, 20133 Milano, Italy*

¹¹*Department of Physics “Aldo Pontremoli”, University of Milano, via Celoria 16, 20133 Milano, Italy*

¹²*Institute of Physics, Faculty of Physics, Astronomy, and Informatics, Nicolaus Copernicus University in Toruń, Grudziadzka 5, 87-100 Toruń, Poland*

¹³*Université Paris-Saclay, CNRS, Laboratoire Aimé Cotton, 91405, Orsay, France.*

¹⁴*Department of Aerospace Science and Technology, Politecnico di Milano, via La Masa 34, 20156 Milano, Italy*

¹⁵*Warsaw University of Technology, Faculty of Physics, ul. Koszykowa 75, 00-662, Warsaw, Poland*

¹⁶*Warsaw University of Technology, Faculty of Electronics and Information Technology, ul. Nowowiejska 15/19, 00-665 Warsaw, Poland*

¹⁷*Czech Technical University, Prague, Břehova 7, 11519 Prague 1, Czech Republic*

¹⁸*Raman Research Institute, C. V. Raman Avenue, Sadashivanagar, Bangalore 560080, India*

¹⁹*Felix Bloch Institute for Solid State Physics, Universität Leipzig, 04103 Leipzig, Germany*

²⁰*The Cockcroft Institute, Daresbury, Warrington WA4 4AD, UK*

²¹*Institute of Physics, Polish Academy of Sciences, Aleja Lotników 32/46, PL-02668 Warsaw, Poland*

²²*INFN Pavia, via Bassi 6, 27100 Pavia, Italy*

²³*Department of Civil, Environmental, Architectural Engineering and Mathematics, University of Brescia, via Branze 43, 25123 Brescia, Italy*

(Dated: October 16, 2023)

We report on laser cooling of a large fraction of positronium (Ps) in free-flight by strongly saturating the 1^3S – 2^3P transition with a broadband, long-pulsed 243 nm alexandrite laser. The ground state Ps cloud is produced in a magnetic and electric field-free environment. We observe two different laser-induced effects. The first effect is an increase in the number of atoms in the ground state after the time Ps has spent in the long-lived 2^3P states. The second effect is the one-dimensional Doppler cooling of Ps, reducing the cloud’s temperature from 380(20) K to 170(20) K. We demonstrate a 58(9) % increase in the coldest fraction of the Ps ensemble.

PACS numbers: 36.10.Dr, 32.80.Pj, 78.70.Bj

Positronium (Ps), discovered in 1951, is the lightest known atomic system, consisting only of an electron and a positron (e^+) [1]. Ps has been extensively studied for its exotic properties as a purely leptonic matter-antimatter system. So far, experiments researching Ps have relied

on formation processes that result in clouds with a large velocity distribution, in the order of several 10^4 m s^{-1} [2–4]. This, for instance, has been limiting the precision of spectroscopy studies due to the large Doppler broadening of the transition lines [5, 6]. The idea of using Ps laser cooling to narrow the velocity distribution dates back to 1988 [7], following the first demonstration of laser cooling on neutral atoms by just a few years [8]. Despite significant efforts [9], Ps laser cooling has not been experimentally achieved yet. A whole range of new fun-

* Corresponding author: brienaeac@liverpool.ac.uk

† Corresponding author: antoine.camper@fys.uio.no

‡ Corresponding author: ruggero.caravita@cern.ch

damental experiments would become feasible with a sufficient amount of cold Ps [10, 11]. These include 1S–2S precision spectroscopy at the 100 kHz level, which will enable testing bound state QED at the $\alpha^7 m_{e^+}$ order [12], measuring the m_{e^+}/m_{e^-} mass ratio with unprecedented accuracy [13], and testing the Equivalence Principle (EP) with a purely leptonic system by looking at the transition red-shift around the Sun’s orbit [14]. Testing the EP with atomic systems consisting of antimatter is the primary goal of the AEgIS collaboration. AEgIS builds on the availability of cold Ps for efficient antihydrogen ($\bar{\text{H}}$) production through the charge exchange reaction $\text{Ps}^* + \bar{\text{p}} \rightarrow \bar{\text{H}}^* + e^-$ between cold antiprotons ($\bar{\text{p}}$) and Ps excited to Rydberg states (Ps^*) [15], first demonstrated experimentally in Ref. [16]. The charge exchange cross-section can be significantly increased by reducing the temperature of the Ps^* cloud [17]. Moreover, forming a Ps Bose-Einstein condensate (BEC) [10, 18] will allow studying stimulated annihilation, producing coherent light in the gamma radiation range [19, 20]. This objective, together with precision spectroscopy, is currently being pursued by the UTokyo group [21], which is actively developing Ps laser cooling with a different methodology employing a chirped laser pulse [22].

Here, we report on the first experimental demonstration of Ps laser cooling by strongly saturating the 1^3S – 2^3P transition for 70 ns, employing an alexandrite-based laser system developed specifically to meet the requirements of Ps laser cooling (high intensity, large bandwidth, long pulse duration). The velocity distributions with and without laser cooling were obtained by Doppler sensitive two-photon resonant ionization along the 1^3S – 3^3P transition [3].

Ps is produced by implanting a bunch of positrons with 3.3 keV kinetic energy into a nanochannel-array etched into a silicon substrate [4, 23]. This e^+/Ps converter is mounted at an angle of 45° with respect to the e^+ beam axis as shown in Fig. 1. About 30 % of the implanted positrons are re-emitted as Ps. An electrostatic buncher [24] with fast potential switching-off [25] complemented by a mu-metal shield were developed to conduct these experiments in a magnetic and electric field-free environment. The measured residual magnetic field was below 1 mT in the Ps production area. This development is important in view of Ps laser cooling, as it was shown that in the intermediate magnetic field range, the saturation of the 1^3S – 2^3P transition leads to a fast annihilation of the atoms due to singlet-triplet state mixing in the excited state manifold [26]. This effect, called “magnetic quenching”, prevents efficient Ps laser cooling [27] and is a strong incentive to work either in the Paschen-Bach regime [28] or, as we do, in a magnetic field-free environment.

The Ps 1^3S – 2^3P transition is driven by the third harmonic of a Q-switched alexandrite laser [29], as proposed in Ref. [10]. The main features of the laser are briefly

summarized hereafter. A pulse length of 70 ns, much longer than the spontaneous emission lifetime of the 1^3S – 2^3P transition (3.19 ns), allows for multiple cooling cycles per pulse. The cavity is 1 m long. The central wavelength is set by means of an intra-cavity Volume Bragg Grating (VBG) [30]. Rotating the VBG finely tunes the fundamental wavelength with an absolute accuracy of 10 pm. Two LBO (lithium triborate) crystals and two BBO (beta barium borate) crystals are used to generate 2.3 mJ at the third harmonic. At 243 nm, the measured root-mean-square (rms) spectral bandwidth is $\sigma_{243} = 101(3)$ GHz. The laser [29] was specifically designed to deliver an irradiance of 100 kW cm^{-2} when focusing 0.7 mJ on an area of 10 mm^2 . As a result, the power on the 20 MHz rms resonance transition line width amounts to $100 \text{ kW cm}^{-2} \times 20 \text{ MHz}/101 \text{ GHz} = 20 \text{ W cm}^{-2}$, much higher than the saturation intensity of the 1^3S – 2^3P transition of 0.45 W cm^{-2} [27]. The laser fluence fills in the spectral gaps in the laser bandwidth [31] and the population in the excited state is saturated within a 360(15) GHz large spectral bandwidth. It should be noted that in these conditions less than 1.4 % of the atoms are photo-ionized [27]. The transverse Doppler profile was probed by fine-tuning the wavelength of a 1.5 ns long 205 nm pulse with a rms spectral bandwidth of $\sigma_{205} = 179(9)$ GHz or 25(1) pm, populating the 3^3P states. A 4 ns long 1064 nm pulse synchronized with the 205 nm pulse induces the photo-ionization of the excited states [32].

The Pockels cell of the alexandrite laser cavity is connected to a high-voltage electronic switch, which is opening and closing the cavity with nanosecond precision to generate a Q-switched pulse featuring a controllable sharp falling edge. Consequently, the laser emission can be suppressed imminent to the arrival of the 205 nm pulse probing the velocity profile, avoiding a temporal overlap of the cooling and probing laser pulses. The 205 nm pulse interacts with Ps about 12 ns after the 243 nm pulse has subsided. This guarantees that all transiently excited Ps atoms have spontaneously decayed to the ground state before probing the velocity distribution of the cloud. The synchronization of the lasers with the e^+ implantation time is achieved with nanosecond time precision by utilizing the ARTIQ/Sinara framework [33] and a LabVIEW-based distributed control system developed at AEgIS [34]. The 243 nm laser beam is co-propagating with the 205 nm (see Fig. 1) and retro-reflected by a dichroic mirror transmitting the 205 nm light. All laser beams are linearly polarized.

The time distribution of the gamma radiation resulting from Ps annihilation, the so-called Single-Shot Positron Annihilation Lifetime Spectroscopy (SS-PALS) [35] spectrum, is acquired in different laser configurations. As illustrated in Fig. 2, the configurations “no lasers”, “205 nm+1064 nm”, “243 nm only”, and “243 nm+205 nm+1064 nm” are used. A $25 \times 25 \text{ mm}$

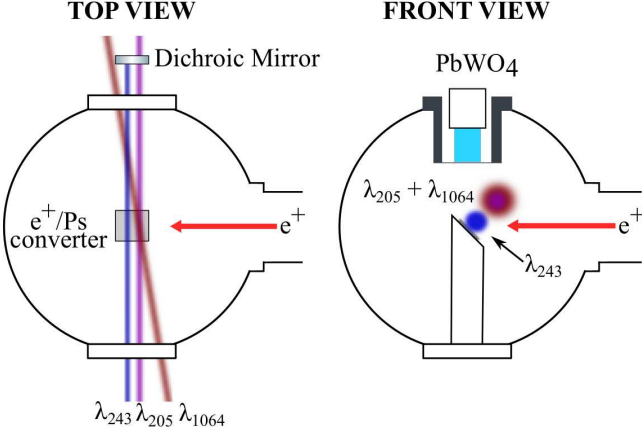


Figure 1. Simplified experimental scheme of the vacuum chamber where Ps is emitted from the e^+ /Ps converter upon e^+ implantation. The cooling laser (λ_{243}) and the two probing lasers pulses (λ_{205} and λ_{1064}) enter and exit the chamber through view-ports. The PbWO₄ crystal is represented in cyan, with the white rectangle above depicting the photo-multiplier tube. The photoionization laser (λ_{1064}) is injected under a slight angle, to avoid laser-induced damage to the dichroic mirror.

PbWO₄ scintillator placed 40 mm above the e^+ /Ps converter and coupled to a Hamamatsu R11265-100 photo-multiplier tube (PMT R11265U-200) connected to an oscilloscope (Teledyne LeCroy HDO4104A), is used to acquire the spectra at a rate of 2.5 GS/s [32].

The long tail in the SSPALS spectrum measured without lasers (black dotted curve), extending from 100 ns to 450 ns in Fig. 2, reflects the 142 ns lifetime of 1^3S Ps in vacuum. Firing the 243 nm laser only, a large fraction of Ps is excited to the 2^3P level, where the annihilation lifetime is much longer than in the ground state. Consequently, the annihilation rate at later times increases (green dash-dotted line in Fig. 2) due to an increase of the number of annihilating atoms in the ground state. By sending only the 205 nm+1064 nm pulses, a fraction of the atoms is selectively photo-ionized. This leads to an immediate small increase in the gamma emission rate due to annihilation of the photo-dissociated e^+ hitting the nearby chamber walls (small bump at 90 ns in Fig. 2), followed by a reduction of the number of ground state Ps annihilating with 142 ns lifetime (red dashed curve). The interaction of the Ps cloud with all three lasers induces a combined effect (blue solid curve in Fig. 2).

In order to study the effects caused by the different laser configurations, S-parameters are constructed as:

$$S = \frac{f_{\text{ON}} - f_{\text{OFF}}}{f_{\text{OFF}}}, \quad (1)$$

where f_{ON} and f_{OFF} denote the integrated SSPALS spectra in the time window between 150 ns and 400 ns. ON refers to one or several of lasers interacting with the Ps cloud, and OFF to no laser interaction. In the follow-

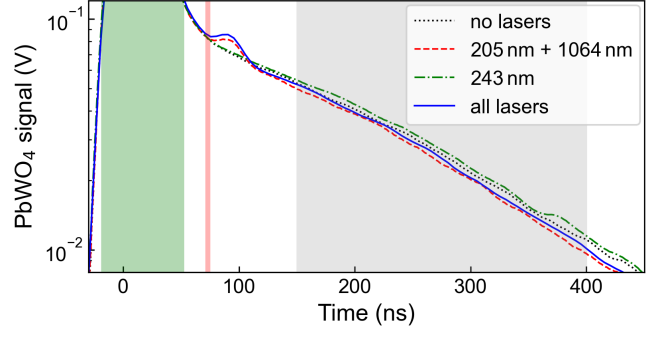


Figure 2. SSPALS spectra of Ps in vacuum without lasers (black dotted curve), 205 nm+1064 nm lasers (red dashed curve), 243 nm laser only (green dash-dotted curve), and all three lasers 243 nm+205 nm+1064 nm (blue solid curve). The 243 nm laser is firing during the time window from -20 ns to 50 ns (green band), while the 205 nm+1064 nm (red vertical line) are injected 75 ns after e^+ implantation time ($t = 0$ ns). Each curve is an average of 90 individual spectra. For analysis, the window between 150 ns and 400 ns (light grey area) was used.

ing, we will refer to $S_{205+1064}$ when only the probing lasers are present, S_{243} when only the cooling laser is present. We further define S_{cool} as the difference between $S_{243+205+1064}$ (when all three lasers are present) and S_{243} :

$$S_{\text{cool}} = S_{243+205+1064} - S_{243} \quad (2)$$

S_{cool} reflects the number of photo-ionized Ps atoms for a given probing laser detuning after interaction with the cooling laser normalized to the number of Ps atoms annihilating in the absence of any laser. High statistics on the S-parameter values is achieved by averaging over sets of spectra acquired consecutively in all the above-mentioned laser configurations. A detrending procedure is applied [36] to correct for slow changes in the amount of Ps produced over time, caused by moderator aging during the long measurement period. A trend function is built by applying Gaussian radial basis regression [37] to the f_{OFF} data. Subsequently, S-parameters are calculated by evaluating the trend function at exactly the time at which the SSPALS spectra with laser(s) are acquired.

First, the Ps velocity distribution without laser cooling was measured by scanning the λ_{205} detuning with the 205 nm and 1064 nm laser beams grazing the surface of the e^+ /Ps converter. In this experiment, the laser pulses were fired 50 ns after the positron implantation time. The transverse Doppler profile, shown in Fig. 3 a), is fitted with a Gaussian function, yielding a rms-width of 44(1) pm. This width corresponds to a Ps rms-velocity of $5.3(2) \times 10^4 \text{ m s}^{-1}$ after de-convolution of the probing laser bandwidth (25(1) pm). The resulting line is centered at $\lambda_{205}^c = 205.044(3) \text{ nm}$, which is compatible with the theoretical value [32].

Secondly, we performed Saturated Absorption Spec-

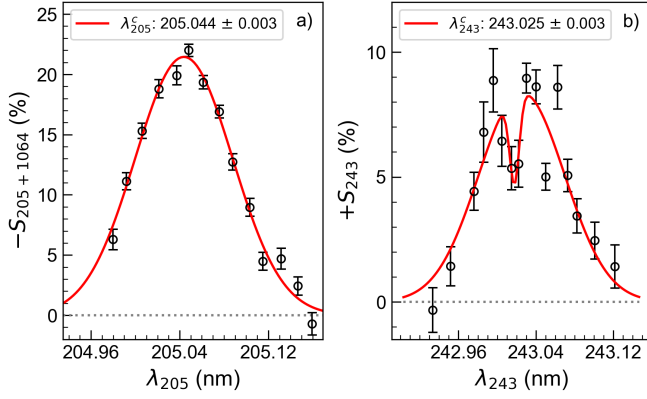


Figure 3. Ps velocity distribution measured by SSPALS. a) Transverse Doppler profile measured by two-photon resonant ionization (205 and 1064 nm lasers) by means of the $S_{205+1064}$ parameter. A Gaussian fit yields a rms-width of 44(1) pm, which translates to a Ps rms-velocity of $5.3(2) \times 10^4 \text{ m s}^{-1}$ after de-convolution of the laser bandwidth. b) Velocity-resolved increase in the number of ground state Ps atoms, induced by the 243 nm transitory excitation to the 2^3P level, represented by the S_{243} parameter. At resonance, the Lamb dip is clearly visible. A 2-Gaussian fit yields a rms-width of the engulfing Gaussian of 44(3) pm, which corresponds to a Ps rms-velocity of $4.9(4) \times 10^4 \text{ m s}^{-1}$.

troscopy on the 1^3S – 2^3P transition [38] to determine the center of the line and the effect of the cooling pulse on the SSPALS spectrum. In Fig. 3 b), SSPALS spectra are recorded as function of the λ_{243} detuning with the cooling laser pulse synchronized with the e^+ implantation time (see Fig. 2). It is worth noting that the resulting S-values are now positive, in contrast to what was observed in the two-photon resonant ionization experiment. To the best of our knowledge, such an increase in the number of ground state Ps atoms caused by a transitory laser excitation to the 2^3P level has never been observed and can be classified as a laser-induced, spectrally tunable preservation of Ps atoms. This effect has to be distinguished from the lifetime enhancement of Ps atoms excited to Rydberg-states [31].

The observed line shape shows a Lamb dip. A 2-Gaussian model is fitted to the data, following the modeling suggested in Ref. [38]. The transition line is centered at $\lambda_{243}^c = 243.025(3) \text{ nm}$, which is in agreement with previous measurements [38]. The engulfing Gaussian features a rms-width of 44(3) pm, which corresponds to a Ps rms-velocity of $4.9(4) \times 10^4 \text{ m s}^{-1}$ after de-convolution of the σ_{243} cooling laser bandwidth (20(1) pm). Hence, this measurement allows to confirm the transverse 1D-velocity profile of our original Ps cloud. Furthermore, the measured width of the Lamb dip is compatible with previous observations [38] and demonstrates the saturation of the 1^3S – 2^3P transition by the laser.

With this understanding of the individual laser interactions with the Ps cloud, we then performed ex-

periments combining the 243 nm cooling laser and the 205 nm+1064 nm probing lasers. The cooling laser remains in the same spatial position, whereas the probing laser beam is moved to a position at a distance of 7 mm from the converter surface (see Fig. 1). Accordingly, the probing laser pulses are delayed by 75 ns with respect to the positron implantation time, as indicated by the red vertical line in Fig. 2. This delay corresponds to the time taken by the atoms in the peak-velocity component of the axial velocity distribution to reach the position of the laser beam.

To characterize the change in the Ps velocity distribution induced by the cooling laser, the detuning of the 243 nm laser is set to -200 GHz (corresponding to $\lambda_{243} = 243.061 \text{ nm}$) and a photo-ionization Doppler scan is performed with the 205 nm+1064 nm lasers. The S_{cool} parameter measured as a function of λ_{205} is shown in Fig. 4. The curve is compared to the $S_{205+1064}$ distribution measured in the same configuration (75 ns delay and 7 mm away from the e^+ /Ps converter), but without prior interaction with the cooling laser. Both of the one-dimensional transverse Doppler profiles were obtained by applying a moving average to the ~ 350 single S-values with a square window (350 GHz in width).

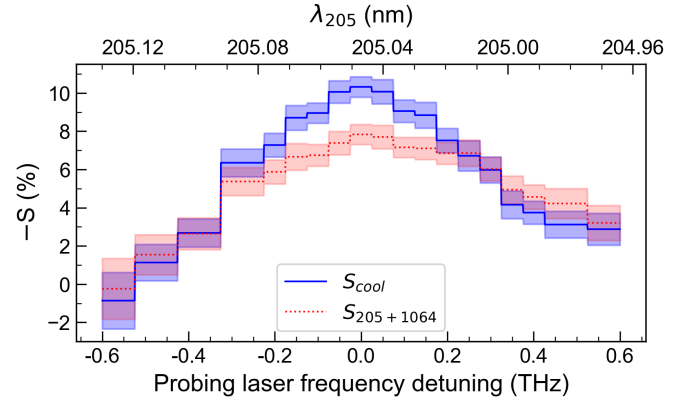


Figure 4. One-dimensional transverse Doppler profiles of the Ps cloud with (solid curve), and without (dotted curve) interaction with the 243 nm cooling laser beam at a fixed frequency detuning of -200 GHz . The semi-transparent bands represent the statistical measurement error (one standard deviation of the average).

The one-dimensional transverse Doppler profile obtained in the presence of the 243 nm cooling laser is narrower than the one measured without it. The asymmetry of the two profiles is caused by a slight increase in the pulse energy of the 205 nm probing laser toward blue-detuned wavelengths. As a first-order estimate of the cooling efficiency, we use a simple Gaussian fit on each of the two distributions to quantify the change in the velocity profile. With prior cooling, we find a rms-width of 269(1) GHz, in contrast to 330(2) GHz without cooling. After de-convolution of the standard deviation of the moving average window ($350 \text{ GHz}/\sqrt{12}$) and of the

σ_{205} laser bandwidth (179 GHz), the Ps rms-velocities corresponding to these widths are $5.4(2) \times 10^4 \text{ m s}^{-1}$, associated with a temperature of 380(20) K, and $3.7(2) \times 10^4 \text{ m s}^{-1}$ associated with 170(20) K, respectively. The obtained rms-velocity in the absence of the cooling laser is in agreement with the result reported in Fig. 3 a) when the 205 and 1064 nm lasers were grazing the target. The interaction with the 70 ns long 243 nm laser pulse reduces the Ps rms-velocity by $1.7(3) \times 10^4 \text{ m s}^{-1}$, corresponding to a temperature reduction of $\Delta T = 210(30) \text{ K}$. The systematic error associated with the arbitrary choice of a Gaussian fitting model is estimated to be $\pm 10 \text{ K}$.

Given the high optical intensity of the 243 nm laser, the average time for all addressed Ps atoms to undergo a single cooling cycle is 6.38 ns [10]. Consequently, with a 70 ns-long Ps-laser interaction, a maximum of 11 cycles is possible. Since the recoil velocity for a single 1^3S – 2^3P transition of Ps is $v_{\text{recoil}} = 1.5 \times 10^3 \text{ m s}^{-1}$ [27], the velocity reduction can reach $11 \times v_{\text{recoil}} = 1.65 \times 10^4 \text{ m s}^{-1}$, corresponding to a temperature reduction of about 200 K, in agreement with our measurements.

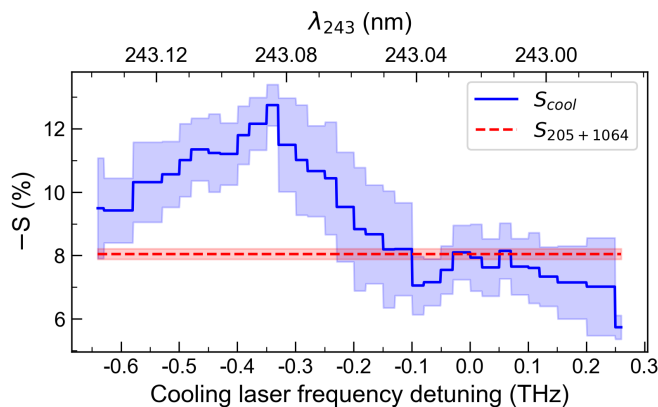


Figure 5. Number of Ps atoms with a velocity within the bandwidth of the 205 nm probing laser, which is kept at resonance, as a function of the cooling laser frequency detuning, normalized to the number of Ps atoms in the absence of all lasers. The dashed horizontal line represents the reference population of Ps atoms in this velocity range with the cooling laser off. The amount of Ps atoms in the center increases by up to 58(9)% at a cooling laser frequency detuning of -350 GHz . The semi-transparent bands represent the statistical uncertainties (one standard deviation of the average).

To evaluate the maximum fraction of fast Ps atoms that can be pushed toward null velocity via recoil effect, the cooling laser detuning was scanned from -0.65 THz to 0.25 THz while the 205 nm laser remained at resonance. The result of this scan is shown in Fig. 5. The horizontal dashed line is the signal measured when only the probing laser interacts with the Ps cloud ($S_{205+1064}$), yielding $-S = 8.0(2) \%$ as the reference for the population near resonance. The blue curve is the S_{cool} parameter as defined in Eq. 2. The curve was obtained by applying a moving average with a window size of 200 GHz. For

a given λ_{243} detuning, the difference between S_{cool} and $S_{205+1064}$ corresponds to the fraction of the Ps population cooled within the bandwidth of the 205 nm laser. A maximum increase of 58(9)% compared to the reference signal is reached at a detuning of -350 GHz .

In conclusion, we have experimentally demonstrated laser cooling of a large fraction of a thermal Ps cloud in a magnetic and electric field-free environment. A temperature decrease from 380(20) K to 170(20) K was observed. Our study also gives an in-depth understanding of the different laser–Ps interactions and their manifestation in the SSPALS spectra recorded during the experiment. In particular, we observed an increase in the number of atoms in the ground state after Ps has been transiently excited to the 2^3P states. As a result, our cooling method has the unique feature of delaying the annihilation, which allows to preserve a large number of Ps atoms while cooling the ensemble. Our results can be improved by adding a second cooling stage with a narrower spectral bandwidth set to a detuning closer to resonance, or by coherent laser cooling [39, 40]. In addition, this technique can be extended to two and three-dimensional laser cooling. The cooling of Ps opens the door to an entirely new range of important fundamental studies with cold Ps beams, including precision spectroscopy, Bose-Einstein condensation of Ps, and tests of the Equivalence Principle with a purely leptonic matter-antimatter system.

Acknowledgement

The authors are grateful to P. Yzombard, C. Zimmer and O. Khalidova for early contributions to this activity, to L. Cabaret for the development of the 1^3S – 2^3P laser and to Dr. S. Cialdi for the original development of the 1^3S – 3^3P laser. This work was supported by the ATTRACT program under grant agreement EU8-ATTPRJ (project O–Possum II); Istituto Nazionale di Fisica Nucleare; European Union’s Horizon 2020 research and innovation programme under the Marie Skłodowska-Curie Grant Agreement No. 754496, FELLINI and No. 748826, ANGRAM; the CERN Fellowship programme and the CERN Doctoral student programme; the EPSRC of UK under grant number EP/X014851/1; Research Council of Norway under Grant Agreement No. 303337 and NorCC; NTNU doctoral program; the Research University – Excellence Initiative of Warsaw University of Technology via the strategic funds of the Priority Research Centre of High Energy Physics and Experimental Techniques; the IDUB POSTDOC programme; the Polish National Science Centre under agreements no. 2022/45/B/ST2/02029, and no. 2022/46/E/ST2/00255, and by the Polish Ministry of Education and Science under agreement no. 2022/WK/06; Marie Skłodowska-Curie Innovative Training Network Fellowship of the European Commission’s

Horizon 2020 Programme (No. 721559 AVA); Wolfgang Gentner Programme of the German Federal Ministry of Education and Research (grant no. 13E18CHA); European Research Council under the European Unions Seventh Framework Program FP7/2007-2013 (Grants Nos. 291242 and 277762); the European Social Fund within the framework of realizing the project, in support of intersectoral mobility and quality enhancement of research teams at Czech Technical University in Prague (Grant No. CZ.1.07/2.3.00/30.0034);

-
- [1] M. Deutsch, Phys. Rev. **82**, 455 (1951).
 - [2] D. Cassidy, P. Crivelli, T. Hisakado, L. Liszkay, V. Meline, P. Perez, H. Tom, and A. J. Mills, Phys. Rev. A **81**, 012715 (2010).
 - [3] M. Antonello et al. (AEgIS Collaboration), Phys. Rev. A **102**, 013101 (2020).
 - [4] S. Mariazzi et al. (AEgIS Collaboration), J. of Phys. B **54**, 085004 (2021).
 - [5] M. S. Fee, A. P. Mills, S. Chu, E. D. Shaw, K. Danzmann, R. J. Chichester, and D. M. Zuckerman, Phys. Rev. Lett. **70**, 1397 (1993).
 - [6] M. S. Fee, S. Chu, A. P. j. Mills, R. J. Chichester, D. M. Zuckerman, E. D. Shaw, and K. Danzmann, Phys. Rev. A **192** (1993).
 - [7] E. P. Liang and C. D. Dermer, Optics Communications **65**, 419 (1988).
 - [8] W. D. Phillips, Rev. Mod. Phys. **70**, 721 (1998).
 - [9] T. Kumita, T. Hirose, M. Irako, K. Kadoya, B. Matsumoto, K. Wada, N. N. Mondal, H. Yabu, K. Kobayashi, and M. Kajita, Nucl. Instrum. Methods Phys. Res. B **171**, 1527 (2002).
 - [10] D. B. Cassidy, H. W. K. Tom, and A. P. Mills, AIP Conference Proceedings **1037**, 66 (2008).
 - [11] D. B. Cassidy, Eur. Phys. J. D **72**, 53 (2018).
 - [12] G. S. Adkins, D. B. Cassidy, and J. Pérez-Rios, Physics Reports **975**, 1 (2022).
 - [13] C. Amsler et al. (Particle Data Group), Physics Letters B **667**, 101 (2008).
 - [14] S. G. Karshenboim, Journal of Physics B: Atomic, Molecular and Optical Physics **49**, 144001 (2016).
 - [15] M. Charlton, Phys. Lett. A **143**, 143 (1990).
 - [16] C. Amsler et al. (AEgIS Collaboration), Communications Physics **4**, 19 (2021).
 - [17] D. Krasnický, R. Caravita, C. Canali, and G. Testera, Phys. Rev. A **94**, 022714 (2016).
 - [18] P. M. Platzman and A. P. Mills, Phys. Rev. B **49**, 454 (1994).
 - [19] A. P. Mills Jr, *Proceedings of the International School of Physics "Enrico Fermi", course 174* (Italian Physical Society, 2010).
 - [20] H. K. Avetissian, A. K. Avetissian, and G. F. Mkrtchian, Phys. Rev. Lett. **113**, 023904 (2014).
 - [21] K. Yamada, Y. Tajima, T. Murayoshi, X. Fan, A. Ishida, T. Namba, S. Asai, M. Kuwata-Gonokami, E. Chae, K. Shu, et al., Phys. Rev. Appl. **16**, 014009 (2021).
 - [22] K. Shu, X. Fan, T. Yamazaki, T. Namba, S. Asai, K. Yoshioka, and M. Kuwata-Gonokami, Journal of Physics B: Atomic, Molecular and Optical Physics **49**, 104001 (2016).
 - [23] S. Mariazzi, P. Bettotti, S. Larcheri, L. Toniutti, and R. S. Brusa, Phys. Rev. B **81**, 235418 (2010).
 - [24] S. Aghion et al. (AEgIS collaboration), Nucl. Instrum. Methods Phys. Res., Sect. B **362**, 86 (2015).
 - [25] S. Aghion et al. (AEgIS collaboration), arXiv p. 1501.01652v2 (2018).
 - [26] K. P. Zioc, C. D. Dermer, R. H. Howell, F. Magnotta, and K. M. Jones, Journal of Physics B: Atomic, Molecular and Optical Physics **23**, 329 (1990).
 - [27] C. Zimmer, P. Yzombard, A. Camper, and D. Comparat, Phys. Rev. A **104**, 023106 (2021).
 - [28] D. B. Cassidy, T. H. Hisakado, H. W. K. Tom, and A. P. Mills, Phys. Rev. Lett. **106**, 173401 (2011).
 - [29] (AEgIS Collaboration), *in preparation*.
 - [30] M. Hemmer, Y. Joly, L. Glebov, M. Bass, and M. Richardson, Opt. Express **17**, 8212 (2009).
 - [31] D. B. Cassidy, T. H. Hisakado, H. W. K. Tom, and A. P. Mills Jr., Phys. Rev. Lett. **108**, 043401 (2012).
 - [32] S. Aghion et al. (AEgIS collaboration), Phys. Rev. A **94**, 012507 (2016).
 - [33] D. Nowicka et al. (AEgIS Collaboration), J. of Phys.: Conf. Ser. **2374**, 012038 (2022).
 - [34] M. Volponi, S. Huck et al. (AEgIS Collaboration), EPJ quantum technology (2023), submitted.
 - [35] D. B. Cassidy, S. H. M. Deng, H. K. M. Tanaka, and A. P. Mills Jr., Appl. Phys. Lett. **88**, 194105 (2006).
 - [36] S. Aghion et al. (AEgIS collaboration), Phys. Rev. A **98**, 013402 (2018).
 - [37] F. Pedregosa, G. Varoquaux, A. Gramfort, V. Michel, B. Thirion, O. Grisel, M. Blondel, P. Prettenhofer, R. Weiss, V. Dubourg, et al., Journal of Machine Learning Research **12**, 2825 (2011).
 - [38] D. B. Cassidy, T. H. Hisakado, H. W. K. Tom, and A. P. Mills, Phys. Rev. Lett. **109**, 073401 (2012).
 - [39] C. Corder, B. Arnold, and H. Metcalf, Phys. Rev. Lett. **114**, 043002 (2015).
 - [40] J. P. Bartolotta, M. A. Norcia, J. R. K. Cline, J. K. Thompson, and M. J. Holland, Phys. Rev. A **98**, 023404 (2018).